The Journal of Neuroscience, September 1991, 11(9): 2938–2946

Axonal Transport Kinetics and Posttranslational Modification of Synapsin I in Mouse Retinal Ganglion Cells

Tamara C. Petrucci,[1] Pompeo Macioce,[1] and Paola Paggi[2]

[1]Laboratorio di Biologia Cellulare, Istituto Superiore di Sanità, 00161 Rome, Italy and [2]Dipartimento di Biologia Cellulare e dello Sviluppo Università "La Sapienza," 00185 Rome, Italy

Synapsin I is a neuron-specific phosphoprotein primarily localized at the presynaptic terminals, where it is thought to play an important role in the mechanisms involved in neurotransmitter release. Its interaction with cytoskeletal proteins and with small synaptic vesicles is regulated *in vitro* by phosphorylation by a calcium/calmodulin-dependent kinase. Here, we present the first evidence that, in the mouse retinal ganglion cells, synapsin I, moving along the axon with the slow component of axonal transport, is phosphorylated *in vivo* at both the head and tail regions. In addition, our data suggest that, after synapsin I has reached the nerve endings, the relative proportion of differently phosphorylated molecules of synapsin I changes, and that these changes lead to a decrease of the overall content of phosphorus. The more basic forms, here collectively referred to as β-forms, become predominant at the terminals after 7 d postlabeling, when the bulk of transported synapsin I has entered the superior colliculus. Along the axon, phosphorylation could be functional in preventing synapsin I from forming, with actin, a dense meshwork that would restrict organelle movement. On the other hand, at the terminals, the dephosphorylation–phosphorylation of synapsin I may regulate the clustering of small synaptic vesicles and modulate neurotransmitter release by controlling the availability of small synaptic vesicles for exocytosis.

Synapsin I appears to be a central component of the linkage of small synaptic vesicles to cytoskeletal elements at the nerve endings, where it plays an important role in the mechanisms involved in modulating neurotransmitter release (De Camilli and Greengard, 1986). Synapsin I comprises two closely related phosphoproteins that arise from a single gene by alternate mRNA processing and differ only in the short COOH-terminal region (Sudhof et al., 1989). Synapsin I is a major substrate for several protein kinases and undergoes multisite phosphorylation. One site in the head region, near the NH_2-terminus, is phosphorylated by cAMP-dependent protein kinase and by calcium/calmodulin-dependent kinase I (CaM I), whereas two sites in the tail region are selectively phosphorylated by calcium/calmodulin-dependent kinase II (CaM II) (Huttner et al., 1981; Kennedy and Greengard, 1981).

In vitro studies have shown that phosphorylation of synapsin I controls its interaction with several cytoskeletal proteins, including microtubules and microfilaments (Baines and Bennett, 1985; Bahler and Greengard, 1987; Petrucci and Morrow, 1987) and its association with small synaptic vesicles (Schiebler et al., 1986). Both interactions with F-actin and synaptic vesicles are affected by phosphorylation of synapsin I on the tail region, whereas phosphorylation on the head site is less effective (Schiebler et al., 1986; Bahler and Greengard, 1987; Petrucci and Morrow, 1987). The participation of synapsin I in the linkage of small synaptic vesicles to the cytoskeleton has been directly shown *in vivo* by freeze-etch electron microscopy (Hirokawa et al., 1989).

Several indications suggest that phosphorylation of synapsin I at the nerve terminal serves to control the binding of synaptic vesicles to actin filaments and the availability of small synaptic vesicles for exocytosis. Phosphorylation-associated translocation of synapsin I from synaptic vesicles/cytoskeleton to cytosol compartment has been observed in response to synaptosomal depolarization (Sihra et al., 1989). The injection of dephosphorylated synapsin I has been shown to decrease neurotransmitter release at the squid giant synapse (Llinas et al., 1985) and to inhibit organelle movement along microtubules within the squid axoplasm (McGuinness et al., 1989).

Synapsin I is synthesized in the neuronal cell body and, together with most axonal and synaptic proteins, conveyed to the synaptic terminals by the process of axonal transport. In the rabbit optic system, the bulk of synapsin I–like molecules moves along the axon with the slow component b (SCb) of the axonal transport, and only a portion is transported with the fast component that carries vesicular structures (Baitinger and Willard, 1987). Therefore, the bulk of synapsin I moves with the cytomatrix components, and the linkage with small synaptic vesicles would occur at the nerve endings.

In this work, we investigated the transport kinetics and the phosphorylation states of synapsin I during the axonal transport and after reaching the nerve endings in the mouse optic system. The results obtained indicate that in mouse retinal ganglion cells synapsin I, transported from the cell body to the nerve terminals at a rate characteristic of the SCb, is phosphorylated both at the head and tail regions. Axonally transported synapsin I appears to comprise several populations of variously phosphorylated molecules. The relative proportion between the acidic or more

Received Jan. 14, 1991; revised Apr. 15, 1991; accepted Apr. 19, 1991.

We wish to thank Dr. Raymond J. Lasek for helpful suggestions and discussions and Gianfranco Macchia and Giulio Berardi for technical assistance. We thank Dr. Enrico Mugnaini for critically reading the manuscript. This work was partially supported by NATO Research Grant 0195/90 to T.C.P., Ministero della Pubblica Istruzione -fondi40%-1989 and -fondi60%-1990 to P.P., and CMR-progetto finalizzato, inrecchiamento to T.C.P. and P.P.

Correspondence should be addressed to Dr. Tamara C. Petrucci, Laboratorio di Biologia Cellulare, Istituto Superiore di Sanità, Vaile Regina Elena 299, 00161, Roma, Italia.

phosphorylated forms (α) and basic or less phorphorylated forms (β) changes in favor of the β-forms at the nerve terminal, but not along the axon. The β-forms appear to be the only ones present when transported synapsin I accumulates at the nerve endings, thus suggesting that they are responsible for binding synaptic vesicles to cytoskeletal structures at the presynaptic terminals.

Materials and Methods

Radiolabeling of retinal ganglion cell proteins, dissection, and preparation of tissue extracts. The retinal ganglion cells were labeled as previously described (Paggi et al., 1989). Briefly, 0.19 mCi of ^{35}S-methionine (specific activity, >800 mCi/mM; New England Nuclear/DuPont) in 1 μl of 0.9% NaCl was injected into the vitreous humor of the right eye of anesthetized male C57Bl/6j mice between 6 and 8 weeks old. The mice were anesthetized and then decapitated at different intervals, ranging from 1 hr to 62 d after the labeling injection. The following segments were collected from the dissected optic system: (1) a 2 mm segment of the right optic nerve (N) extending between 3 and 5 mm from the posterior scleral surface of the eye, (2) a 2 mm segment of the left optic tract (T) extending between 6 and 8 mm from the posterior scleral surface of the eye, and (3) the left superior colliculus (SC), which is 11–13 mm from the posterior scleral surface of the eye. The optic nerve (N) and tract (T) segments contain the axons of the retinal ganglion cells, and the superior colliculus (SC) segment contains these axons and their terminals. Corresponding segments removed from 8–10 mice, killed at each postinjection interval, were pooled and homogenized in 200 μl of BUST (0.1 M Tris, pH 6.8, 2% β-mercaptoethanol, 8 M urea, 1% SDS) with a ground-glass microhomogenizer and sonicated for 1 min. Homogenates were then centrifuged at 22,000 × g for 20 min at room temperature. A measured aliquot of each supernatant, to which purified mouse synapsin I was added as internal standard, was analyzed by two-dimensional (2-D) nonequilibrium pH/SDS-polyacrylamide gel electrophoresis (NEPHGE/SDS-PAGE). As previously described (Paggi et al., 1989), to deal with the unavoidable variability in the amount of labeled amino acid incorporated into the proteins of the retinal ganglion cells of different animals, we introduced an a priori correction. We pooled only those preparations in which we achieved at least 30% of the maximum limit in the total radioactive protein labeling of the optic nerve. The most heavily labeled animal was taken as our best estimate of the maximal limit, and the chiasm of each dissected optic system was used to determine the total radioactive proteins. This a priori correction (Fisher, 1966) obviates any requirement for further normalization of the results and permits the direct comparison of data from 2-D-NEPHGE/SDS-PAGE analysis.

Electrophoresis and fluorography. 2-D-NEPHGE/SDS-PAGE was performed according to O'Farrel (1975) employing the standard range of ampholine (pH 3–7 and 5–7; LKB Instruments) and 8% acrylamide slab gels (Laemmli, 1970). The molecular-mass standards used were (expressed as kDa) β-galactosidase (116), phosphorylase b (97), bovine serum albumin (66), ovalbumin (45), and carbonic anydrase (29). Gels were stained with 0.5% Coomassie blue in 10% acetic acid and 15% methanol. The radioactive polypeptides were visualized by fluorography according to the method of Bonner and Laskey (1974) and Laskey and Mills (1975) using XR-5 x-ray film (Kodak) stored at −70°C.

Quantitation of radioactivity of transported synapsin I. Regions of 2-D gel corresponding to synapsin Ia and Ib were excised using both the fluorograph to locate the position of the labeled polypeptides on gel and the Coomassie blue–stained spots of purified synapsin I. Gel slices were solubilized (Paggi et al., 1989), and the radioactivity was quantified by liquid scintillation counting using Optifluor (Packard) as scintillant. Counts were corrected for quenching and were converted to disintegrations per minute (dpm). Radioactivity values at each postinjection time were corrected for ^{35}S-methionine decay. According to the "window" method of analysis (Paggi et al., 1989), data for individual segments (N, T, SC) were plotted as a function of the interval between labeling injection and collection of the segments for analysis. Synapsin I associated radioactivity was also determined by densitometry of 2-D fluorographs (Ultroscan II, LKB).

Determination of the pulse-transient. The pulse-transient (Paggi and Lasek, 1987; Paggi et al., 1989, 1990) is a mathematical summary of the transport curve through an axonal window: it is the area under the curve of radioactivity versus time. In any axonal window, the pulse-transient is determined by (1) the length of the segment, (2) the total amount of radioactivity in the pulse-labeled wave, and (3) the rate of which the pulse-labeled wave enters, traverses, and exits the segment (Paggi and Lasek, 1987). It is then a measure of all radioactivity associated to a specific protein that entered and cleared the axonal window during the postlabeling period of observation. As previously reported (Paggi et al., 1989, 1990), to compare the pulse-transient of the optic nerve segment with that of the the optic tract and of the superior colliculus segments, values for the optic tract and the superior colliculus were corrected taking into account the percentage of retinal ganglion cell axons uncrossed at the optic chiasm and the percentage of axons projecting to the lateral geniculate nucleus rather than to the superior colliculus.

Determination of the median transit time. The median transit time is a way of quantitatively summarizing the rate of transport of labeled protein. It is the postlabeling time required for 50% of a specific radiolabeled protein to traverse and clear a given segment of axon. It is calculated by integrating the part of the area under the curve of radioactivity versus time, so that the area equals 50% of the pulse-transient.

Phosphorylation of proteins in vivo. Mice were injected into the vitreous of the eye with 100 μCi of ^{32}P-orthophosphate (specific activity, >8500 Ci/mM; DuPont) as described above. The mice were killed 2 d after the injection. Right optic nerves (N), left optic tracts (T), and the left superior colliculi (SC) were collected from the dissected optic system of 13 mice. Samples were homogenized, and phosphorylated proteins were separated by 2-D-NEPHGE/SDS-PAGE as described above. The radioactive polypeptides were visualized by autoradiography using XR-5 x-ray film stored at −70°C. The labeled synapsin I was quantified by densitometry.

Cystein specific cleavage of axonally transported proteins by S-cyanylation. Mice were injected in both eyes with 100 μCi of ^{32}P phosphate (specific activity, >8500 Ci/mM; DuPont), and the optic system was dissected 2 d later. Purified bovine synapsin I (1 mg; see below) was added to 1 ml homogenate sample obtained by homogenizing segments from the left and right optic nerves and optic tracts of 15 mice. The homogenate sample, dialyzed against 7.5 M guanidine-HCl, 25 mM Tris-HCl, 1 mM EDTA, and pH 8.5 buffer, was cleaved with 2 mM 2-nitro-5-thiocyanobenzoic acid (NTCB; Sigma) at 37°C for 24 hr (Petrucci and Morrow, 1987). The resulting peptide mixture was dialyzed in 10 mM Tris-HCl, 1 mM EDTA, 0.1 mM β-mercaptoethanol, and pH 8.5 buffer, lyophilized, and analyzed by 2-D-NEPHGE/SDS-PAGE. The labeled peptides were visualized as indicated above.

Synapsin I purification. Synapsin I was purified from either bovine or mouse frozen brains by acidic extraction, followed by ion-exchange chromatography on CM-cellulose (Whatman) and hydroxylapatite (BioRad) as previously described (Petrucci and Morrow, 1987). No differences were found in the biochemical properties and electrophoretic behavior of synapsin I from the two sources.

Dephosphorylation of phosphoproteins. ^{35}S-labeled proteins from the optic nerve, optic tract, and superior colliculus segments of 10 mice 2 d postinjection and the superior colliculi of 10 mice 14 d after labeling were homogenized in 300 μl buffer [50 mM Tris-HCl, pH 8.0, 100 mM NaCl, 1 mM $ZnSO_4$, 2.5 mM phenylmethylsulfonyl fluoride (PMSF), 100 μg/ml leupeptin, 0.1% aprotinin], respectively. Each sample, divided in two aliquots, was incubated with and without 150 U of bovine alkaline phosphatase (Sigma) at 33°C for 18 hr. Proteins were precipitated with cold acetone and analyzed by 2-D-NEPHGE/SDS-PAGE. The labeled peptides were visualized by fluorography as specified above.

Results

Transport kinetics of synapsin I

We have quantified ^{35}S-methionine labeled synapsin Ia and Ib in the N, T, and SC segments from more than 350 optic systems of mice killed at 1, 3, and 6 hr and 1, 2, 4, 7, 14, 22, 36, and 62 d after labeling. Figure 1*A* shows a representative fluorograph of ^{35}S-methionine–labeled proteins separated by 2-D-NEPHGE/SDS-PAGE from SC 14 d after labeling.

To study the transport kinetics of synapsin I, the amounts of radioactivity present in the synapsin Ia and Ib spots were quantified by liquid scintillation spectroscopy and/or densitometry, and the results were then plotted as a function of postlabeling time. In a pilot experiment, we attempted to examine the pro-

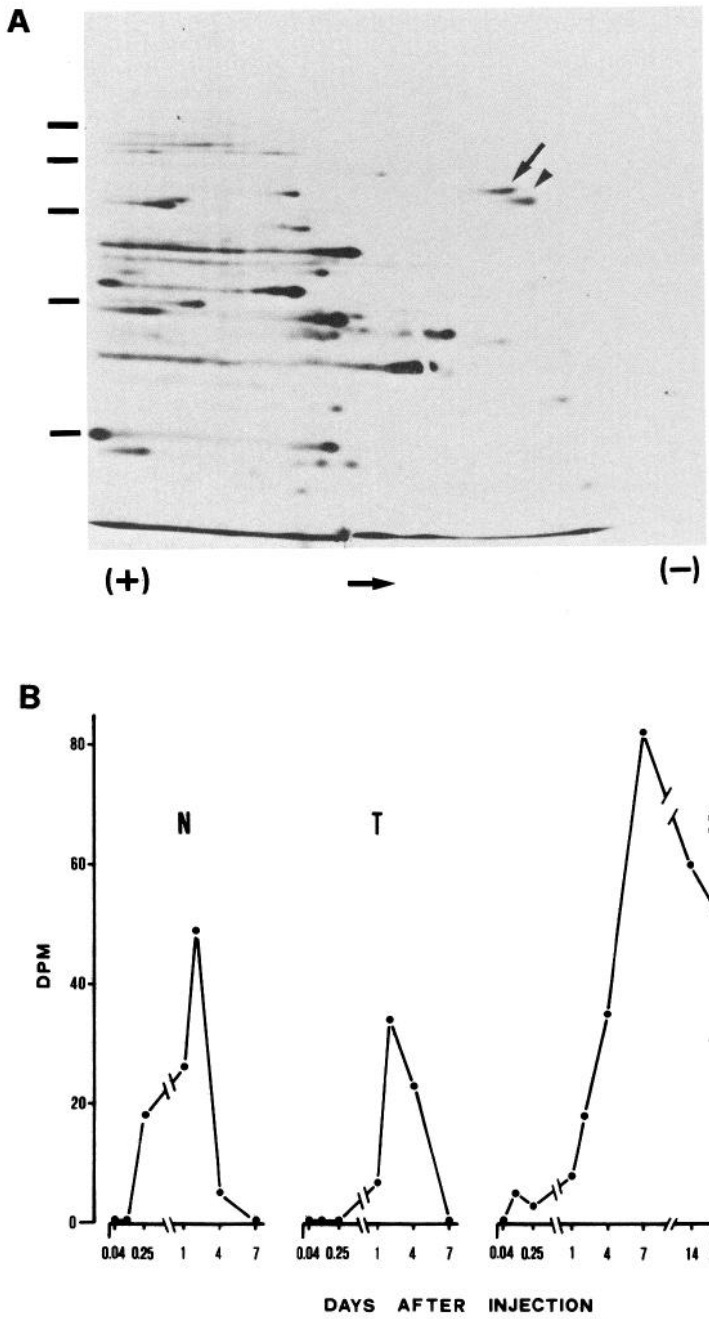

Figure 1. A, Representative fluorograph showing labeled polypeptides from the SC separated by 2-D-NEPHGE/SDS-PAGE 14 d after labeling the retinal ganglion cells. Spots corresponding to synapsin Ia (*arrow*) and Ib (*arrowhead*) are indicated. The mobility of molecular-mass standards, 116, 97, 66, 45, and 29 kDa (*top* to *bottom*), is shown by the *bars* on the *left*. The acidic (+) and the basic (−) portions of the gel are indicated. *B,* Axonal transport kinetics of ^{35}S-methionine synapsin I after labeling of retinal ganglion cells. Fluorographs such as in *A* were used to remove the gel regions containing synapsin I. Data from 2 mm of the *N* segment, the *T* segment, and the *SC* are plotted as a function of the time interval between injection of the radioactive precursor and collection of the segments for analysis. Data points are the average of two or three observations, and each observation is a pool of 10 mice killed at 1, 3, and 6 hr and 1, 2, 4, 7, 14, 22, 36, and 62 d for a total of more than 350 animals. The curves are asymmetric, showing a rapid raising phase that reaches a peak at 2, 2, and 7 d in N, T, and SC, respectively. The declining phase approaches background level of radioactivity by 7 d in N and T, while in SC it has not yet reached background level of radioactivity at 62 d.

portion of transported ^{35}S-methionine–labeled synapsin Ia and Ib. The relative amounts, however, were not sufficient to quantify the two components properly (data not shown). Figure 1*B* shows the transport kinetics curves of radiolabeled synapsin I through three different windows of the optic system. The windows are retinal ganglion cell axon segments: the N and the T segments contain axons and extended 3–5 and 6–8 mm, respectively, from the posterior surface of the eye ball; the SC segment contains axons and their terminals and is located 11–13 mm from the posterior surface of the eyeball.

The general shapes of synapsin I transport curves through N, T, and SC segments are similar to those for other SCb proteins (Paggi et al., 1989, 1990): they are asymmetric and unimodal. The rising phase of the curve, which reflects the entrance of components into the axon segment, reaches a peak that is followed by a declining phase of radioactivity, reflecting the exit of proteins from the axon segment. The N and T curves reach a background level at 7 d postinjection: this indicates that no radiolabeled synapsin I is permanently deposited within the axon segments. On the contrary, the SC curve, as already observed for other SCb proteins, has not yet reached background level of radioactivity at 62 d. These observations indicate different transit rates for synapsin I in N and in T, which contain only the retinal ganglion cells axons, and in SC, which contains axons and their terminals (see next section).

Rate of transport of synapsin I

Labeled synapsin I entered N, T, and SC segments between 3 and 6, 6 and 24, and 1 and 3 hr, respectively (Fig. 1*B*). The radioactivity reached a peak at 2 d both in N and in T, and at

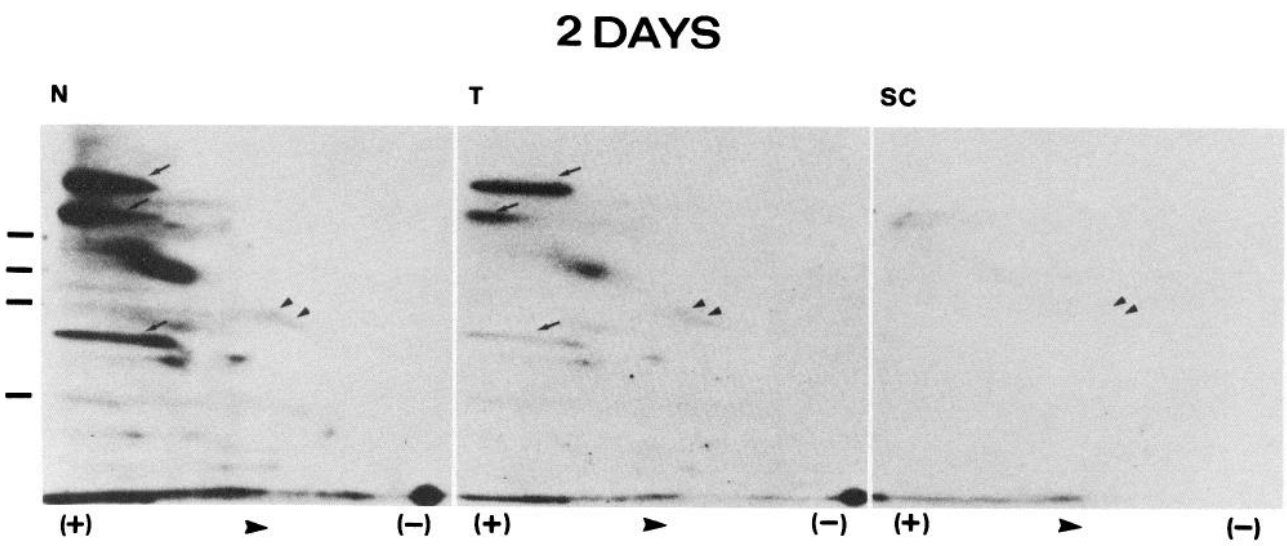

Figure 2. **Phosphorylated synapsin I is transported down the axon. Autoradiographs of axonally transported ^{32}P-labeled proteins of rat *N* segment, *T*, and *SC* separated by 2-D-NEPHGE/SDS-PAGE 2 d after labeling of retinal ganglion cells. Spots corresponding to synapsin Ia and Ib (*arrowheads*) and neurofilament peptides (*arrows*) are indicated. The *bars* to the *left* correspond to the position of the molecular-mass standards described in Figure 1*A*. The acidic (+) and basic (−) portions of the gel are indicated.**

7 d in SC. The T peak was much broader than the N peak. In fact, at 4 d the radioactivity in N and T was about 10% and 68% of the respective maximum peak. From our data, we cannot determine exactly when the radioactivity peaked. However, from the position of the observed peak, the actual maximum should occur later in the tract (between 2 and 4 d) than in the nerve (about 2 d). Therefore, from the position of the observed peak in the three windows, we can estimate a peak rate of transport of 1.5–3 mm/d. This rate of transport indicates that synapsin I is associated with the SCb complex of proteins (Paggi et al., 1989, 1990). We could not detect any labeled synapsin I 1 hr after the labeling either in the retinal ganglion cell axon segments, N and T, or at their terminals in SC. The presence of barely detectable labeled synapsin I in SC 3 hr after labeling (Fig. 1*B*), before its appearance in N and T, indicates that fast transported synapsin I constitutes, at most, only a small pool. To show the presence of fast-transported synapsin I in N and T, observations at postlabeling times shorter than 1 hr would eventually be required. However, if the ratio fast-transported/slow-transported synapsin I in mouse retinal ganglion cells is the same as that observed in rabbit retinal ganglion cells (Baitinger and Willard, 1987), the amount of fast-transported synapsin I in the axon would be below the level detectable by our methods of analysis.

Median transit time of synapsin I

As already observed for other SCb proteins (Paggi et al., 1989, 1990), synapsin I pulse-labeled wave broadens while advancing along the axons (Fig. 1*B*). This spreading (Paggi et al., 1989, 1990) appears to be a consequence of the different transport rates present even among otherwise identical molecules. One way to summarize these different rates quantitatively is to evaluate the median transit time, which is the time required for 50% of the window-analysis wave to pass from the retina into and through a given segment (Paggi et al., 1989). In N and T, where synapsin I is transported through the axons of the retinal ganglion cells by axonal transport mechanisms, the median transit time reflects the clearance of the axonal segments operated by these mechanisms. In SC, where both axons and their terminals are present, the median transit time reflects the clearance from the segment by specific removal mechanisms operating at the nerve endings as well as the rate of transport into the terminals.

The median transit time in N, T, and SC were 2, 3, and 20.5 d, respectively. This corresponds to a median transit rate of 1.5–2 mm/d in N and T, the axon proper segments, and of 0.54 mm/d in SC, the segment containing both axons and terminals. In SC, the actual median transit time is probably longer than 20.5 d; in fact, at 62 d after injection, the labeled synapsin I had not yet cleared the SC segment (Fig. 1*B*). The actual median transit time calculated after extrapolation to 0 of the SC curve was 29 d, corresponding to a median transit rate of 0.38 mm/d. The median transit time in SC was 925% and 583% longer than that observed in N and T segments, respectively.

Pulse-transient of synapsin I

Figure 1*B* shows that the amplitude of the transport curves for N, T, and SC is different. To quantify these differences, we calculated the pulse-transients. The pulse-transient represents the area under the window-analysis transport curve, and it is a measure of the radioactive synapsin I that entered and cleared the axonal window, N, T, and SC, during the postlabeling period of observation. The pulse-transient was 961 and 899 dpm/d for N and T, respectively, and it was 23,075 dpm/d for SC. Both the long residence time and the higher pulse-transient in SC than in N and T conform with the higher amount of synapsin I detected in the terminal regions than in axons by immunogold labeling technique (De Camilli et al., 1983) and with the prevalent functional role suggested for synapsin I at nerve endings.

Phosphorylation of axonally transported synapsin I

Phosphorylation of synapsin I has been shown to regulate interaction of the protein molecules with actin filaments (Bahler and Greengard, 1987; Petrucci and Morrow, 1987). Because synapsin I is transported with the SCb, which comprises cytomatrix proteins including actin, we investigated the phosphor-

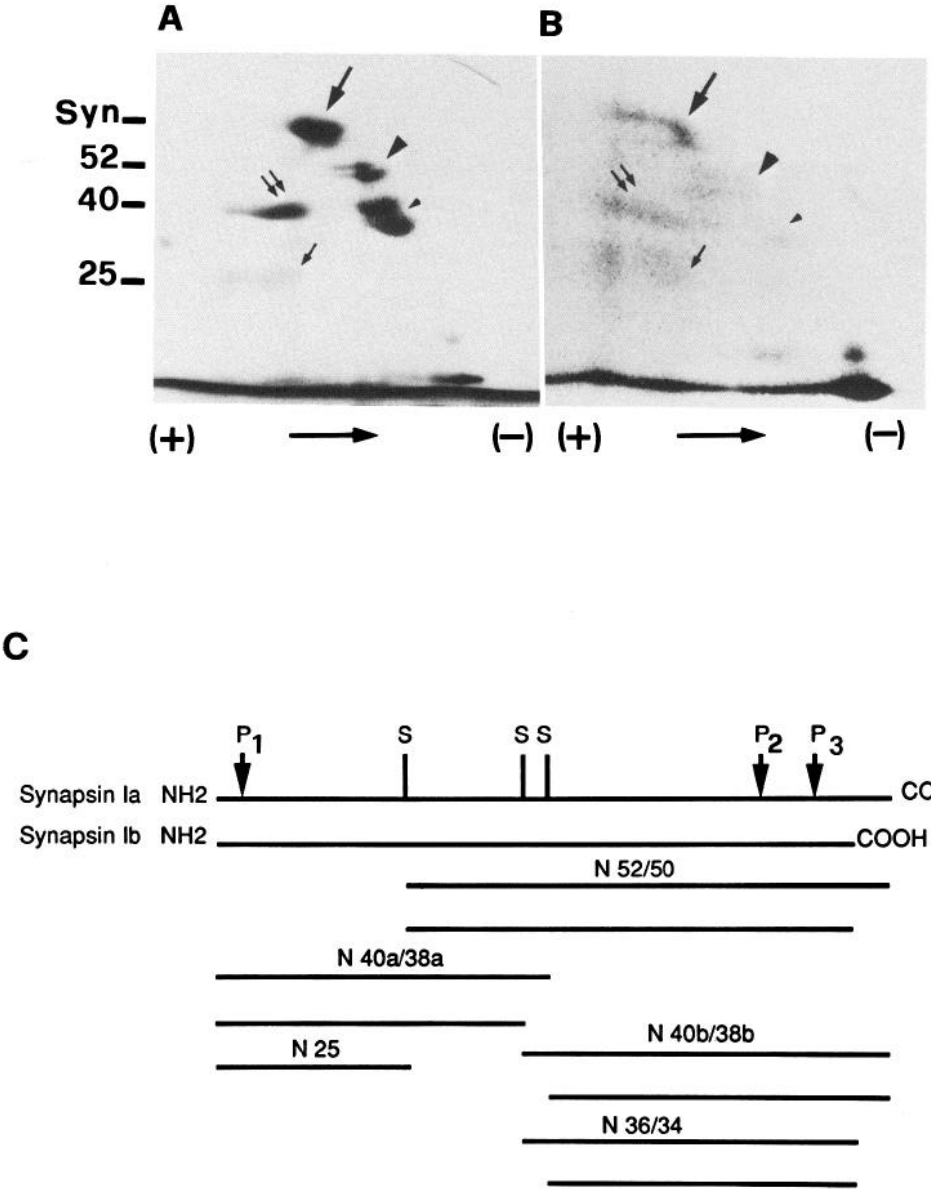

Figure 3. Identification of the phosphorylated sites in axonally transported synapsin I. Purified synapsin I was added to ^{32}P-labeled axonally transported polypeptides and then subjected to NTCB cleavage. Analysis of the NTCB digestion mixture by 2-D-NEPHGE/SDS-PAGE is indicated by Coomassie blue staining (*A*) and by autoradiography (*B*). The spots corresponding to intact synapsin I (*large arrows*), NTCB-derived peptides N52/50 (*large arrowheads*), N40a (*double arrows*), N40b and N36/34 (*small arrowheads*), and N25 (*small arrows*) are indicated. All NTCB-derived peptides that comprise the amino- or carboxy-terminal of synapsin I were radioactively labeled. The acidic (+) or basic (−) portions of the gel are indicated. *C,* The relationship of NTCB-derived peptides and intact synapsin Ia and Ib is shown. The position of phosphorylated sites (P_{1-3}) and the cysteine residues (*S*) of the molecule are shown. The NH_2-terminal region of synapsin I comprises site P_1 phosphorylated by cAMP-dependent protein kinase and CaM I. Sites P_2 and P_3, near the COOH-terminus of the molecule, are phosphorylated by CaM II.

ylation state of synapsin I during axonal transport by labeling mouse retinal ganglion cells with ^{32}P-orthophosphate *in vivo.* Only three sites per molecule can be phosphorylated in synapsin I (Huttner et al., 1981), and in order to detect the ^{32}P-labeled protein, the segment window of N and T was larger than the 2 mm window used to measure the transport kinetics of ^{35}S-labeled synapsin I. Figure 2 shows that, 2 d after the labeling, synapsin I moving through N, T, and SC segments was labeled. At this postinjection time, ^{32}P- or ^{35}S-labeled synapsin I was detectable in all segments (Figs. 1*B,* 2), and the relative amounts of phosphorylated synapsin I in N, T, and SC were comparable with the relative amounts of ^{35}S-labeled synapsin I in these segments. This finding indicates that synapsin I remains phosphorylated as it is transported along the axon and when it enters the nerve terminals. Moreover, 14 d after the injection, when ^{35}S-labeled synapsin I is present in the superior colliculus in a very high amount (see Fig. 1*B*), no ^{32}P-labeled synapsin I was detected in SC (data not shown). This observation suggests that, after synapsin I has entered the nerve terminals in the superior colliculus, the initially incorporated phosphate groups of synapsin I are turned over.

Identification of the phosphorylated sites of axonally transported synapsin I

Synapsin I can be phosphorylated at different sites, in the "head region" by cAMP-dependent protein kinase and CaM I (Huttner et al., 1981; Kennedy and Greengard, 1981) and in the "tail" region by CaM II kinase (Huttner et al., 1981; Kennedy and Greengard, 1981). Phosphorylation on the tail region inhibits the ability of synapsin I to bundle F-actin and decreases the linkage to small synaptic vesicles (Schiebler et al., 1986; Bahler and Greengard, 1987; Petrucci and Morrow, 1987).

In order to determine which sites of axonally transported synapsin I were phosphorylated, ^{32}P-labeled proteins from the optic nerve and optic tract were subjected to chemical cleavage by the cystein-specific reagent NTCB and analyzed by 2-D-NEPHGE/SDS-PAGE (Fig. 3). Coomassie blue staining (Fig. 3*A*) and autoradiography (Fig. 3*B*) showed spots, previously

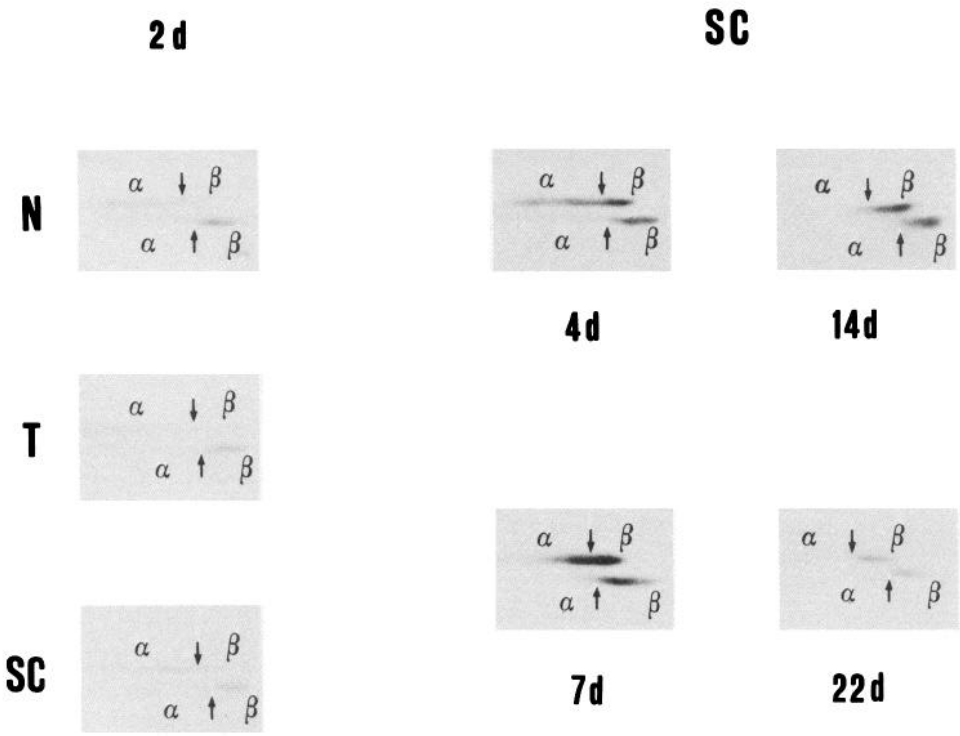

Figure 4. Neuronal region–dependent change and time-dependent change in the spots morphology of axonally transported ^{35}S-methionine labeled synapsin I. Fluorographs of 2-D-NEPHGE/SDS-PAGE of the regions corresponding to ^{35}S-labeled synapsin Ia and Ib from samples obtained from the *N* and *T* 2 d after injection, and from the *SC* 2, 4, 7, 14, and 22 d after injection. The *arrows* indicate the arbitrary boundary between the acidic and the basic forms of synapsin I. The acidic forms of synapsin I, collectively labeled α, are characteristic of the nerve fiber. The more basic forms, labeled β, are predominant at the nerve endings after all the radioactive synapsin I has entered the terminals.

identified (Petrucci et al., 1988) as intact synapsin I, and NTCB-derived peptides N52/50, N40a, N40b, N36/34, and N25/23. The relationship between NTCB-derived peptides and the parent molecules (Bahler et al., 1989; Petrucci and Morrow, 1991) is shown in Figure 3*C*. Intact synapsin I and all major NTCB-derived peptides comprising either the amino-terminus or the carboxy-terminus were labeled (Fig. 3*B*), indicating that axonally transported synapsin I was phosphorylated on both the head and tail regions.

The tail region comprises two sites of phosphorylation (Huttner et al., 1981; Sihra et al., 1989), and the radiolabeling signal of carboxy-terminal peptides (N52/50, N40b, and N36/34) would be expected stronger than that of amino-terminal fragments. On the contrary, the signal of radioactivity of carboxy-terminal peptides seems to be ligher (Fig. 3*B*). We could not determine the specific activity of each peptide because of the very low amount of labeling. One explanation could be that, in our system, only one site is phosphorylated in the tail region. Alternatively, the radioactivity signal of amino-terminal fragments may be artifactually strengthened because of the inherent higher background present in the acidic portion of the gel.

Different population of phosphorylated synapsin I

A neuronal region–dependent change and a time-dependent change in the electrophoretic resolution of axonally transported ^{35}S-labeled synapsin I were observed. Figure 4 shows the fluorographs of 2-D-NEPHGE/SDS-PAGE of the region corresponding to ^{35}S-labeled synapsin Ia and Ib in N, T, and SC. Samples were obtained from the optic nerve and tract 2 d after injection, and from the superior colliculus 2, 4, 7, 14, and 22 d after injection. Synapsin I spots on 2-D gels of N and T and SC segments appeared as streaks with a rather uniform intensity in which individual spots were indiscernible (Fig. 4, 2d). The more basic forms of ^{35}S-labeled synapsin I were the only components present in SC after radioactively labeled synapsin I had cleared the axon segments and entered the terminals (Fig. 4, SC, 14d and 22d) and are termed here β-forms. An arbitrary boundary was chosen to distinguish the more acidic forms of synapsin I, termed α-forms, which were present in the axons together with the more basic β-forms (Fig. 4).

We can exclude the possibility that the observed change in the electrophoretic resolution of ^{35}S-labeled synapsin I between the axon (N and T) and nerve terminal (SC) segments is due to variability in the electrophoretic system used: the pattern observed was reproducible, and the resolution of spots of purified synapsin I, added to samples as internal standard, did not change (see Fig. 3*A*, intact synapsin I). Furthermore, when cold synapsin I was detected from the superior colliculus by Western blot and affinity-purified polyclonal antibodies against synapsin I, it showed a spot morphology (data not shown) similar to that shown in SC by ^{35}S-labeled synapsin I 14, 22, 36, and 62 d postinjection. Moreover, the spot morphology was similar to that of standard purified synapsin I, which is dephosphorylated (Petrucci and Morrow, 1987). These considerations suggest that the fraction of synapsin I accumulated at the synaptic terminals becomes indistinguishable from synapsin I endogenous to the SC segment.

The neuronal region–dependent change and time-dependent change in the electrophoretic resolution of synapsin I spots may be due to the presence of several populations of molecules with different degrees of phosphorylation and to the removal of phosphate from some or all sites of synapsin I after it has reached the nerve endings. In order to test this possibility, ^{35}S-labeled proteins prepared from the optic nerve, optic tract, and the superior colliculus 2 d postinjection and from the superior colliculus 14 d after labeling were incubated with alkaline phosphatase. Figure 5 shows the fluorographs of 2-D-NEPHGE/SDS-PAGE of the region comprising ^{35}S-labeled synapsin I in

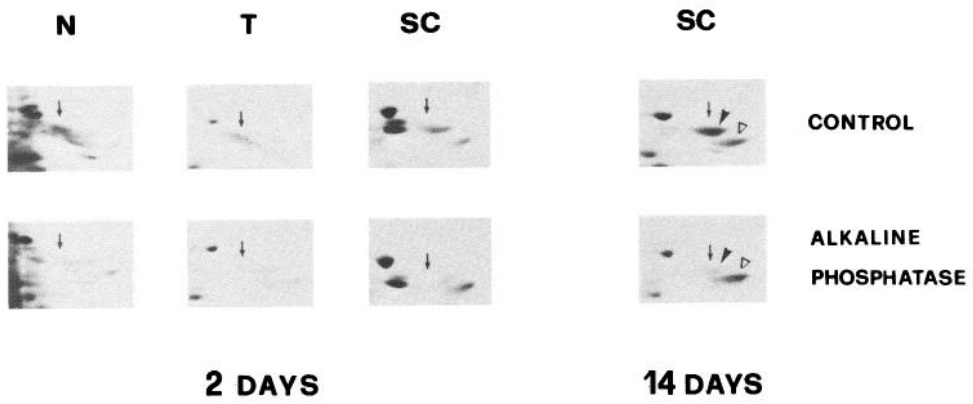

Figure 5. Fluorographs of 2-D-NEPHGE/SDS-PAGE of the regions corresponding to ^{35}S-labeled synapsin Ia and Ib from samples obtained from the *N* and *T* 2 d after injection and from the *SC* 2 and 14 d after injection and incubated with or without alkaline phosphatase at 33°C for 18 hr. The *arrows* in each *pair* of samples, control and alkaline phosphatase–treated, allow us to visualize the disappearance of the more acidic forms of synapsin I, the α-forms, in the samples (*N, T,* and *SC, 2 days*) after alkaline phosphatase digestion. In *SC 14 days* postinjection, after treatment with alkaline phosphatase, proteolytic activity reduces the densities of spots corresponding to synapsin Ia (*solid arrowhead*) and to other proteins (*left side,* unlabeled), but it does not alter the form of the synapsin Ia spot. The form and density of the synapsin Ib spot (*open arrowhead*) are not substantially changed.

control and alkaline phosphatase–treated samples analyzed in parallel. After treatment with alkaline phosphatase the most acidic part of synapsin I spots, the α-forms, disappeared in N, T, and SC 2 d postinjection (Fig. 5). Although a mixture of protease inhibitors was always present in the samples during the alkaline phosphatase digestion, we observed that proteolytic activity slightly affected the spot density of some proteins including synapsin I, and synapsin Ia more than synapsin Ib.

By contrast, when ^{35}S-labeled proteins from the superior colliculus 14 d after labeling were incubated with alkaline phosphatase, no evident differences in the electrophoretic resolution of ^{35}S-labeled synapsin I spots were observed (Fig. 5). In the alkaline phosphatase–treated SC sample of Figure 5 (14 d), the spot densities of synapsin Ia and other proteins present in the selected area of the gel were also slightly affected by proteolytic activity.

Discussion

Transport kinetics of synapsin I

To follow the movement and posttranslational modification of synapsin I in the mouse optic system, the proteins were labeled as a pulse in the retinal ganglion cells. Radioactive synapsin I was measured by 2-D-NEPHGE/SDS-PAGE in N, T, and SC segments or windows. The N and T windows, located at a distance of 3–5 and 6–8 mm, respectively, from the posterior surface of the eyeball, provide a view of the synapsin I moving through the axon shafts; the SC provides a view of synapsin I at the preterminal and terminal regions. Our results show that, in the mouse optic system, synapsin I is principally transported with the SCb of the axonal transport as indicated by the peak rate of transport (1.5–3 mm/d) calculated on the basis of the observed peak in the N, T, and SC windows.

Detailed studies have revealed differences in the transport kinetics of SCb proteins (Garner, 1979; Garner and Lasek, 1982; Paggi et al., 1989). The present data show that synapsin I is characterized by an overall transport rate that is faster than that previously reported for the faster-moving SCb proteins such as clathrin (Paggi et al., 1989). In fact, synapsin I has already cleared the N and T windows between 4 and 7 d postinjection, while clathrin was found moving through the same windows more than 21 d after labeling (Paggi et al., 1989). Moreover, synapsin I median transit time through N and T windows was about four times faster than that previously reported for clathrin (Paggi et al., 1989).

In addition, it is important to point out that, as previously observed for clathrin (Paggi et al., 1989), the synapsin I pulse-transients in the N and T windows remain essentially unchanged as the protein moves distally along the axon, that is, from N to T. This indicates that synapsin I is not degraded or deposited along the axons. The constancy of the pulse-transient in N and T might reflect the fact that both synapsin I and clathrin are proteins essentially devoted to nerve terminals, where they are associated to two different types of vesicles, the small synaptic vesicles (De Camilli et al., 1983; Hirokawa et al., 1989), and the coated vesicles (Pearse, 1976), respectively.

In the present experiments, we found that in the SC window, which contains both the axons of retinal ganglion cells and their terminals, the median transit time was one order of magnitude higher and the pulse-transient was about 20 times higher than those detected in N and T windows. The median transit time and the pulse-transient are measures of protein residence time (Paggi and Lasek, 1987; Paggi et al., 1989, 1990). In any axon segment, the residence time of an axonally transported protein is determined by the rate of entry, transit, and exit of the protein through the segment; it is therefore controlled by the axonal transport mechanisms. In segments containing both axon terminals and shafts, such as the superior colliculus, the clearance of the proteins is controlled not only by the rate of transport but also by the local degradation mechanisms, which operate selectively on each protein at the terminals. In fact, different residence times have been found for proteins whose rate of transport along the axons is the same (Paggi et al., 1990). These differences from protein to protein cannot be fully accounted for by a uniform slowing of the rate of transport at the nerve endings. Therefore, the larger residence time at the nerve endings for synapsin I than for other proteins such as neurofilament proteins (Paggi and Lasek, 1987) suggests that the degrading mechanism operates slower on synapsin I than on neurofilament proteins.

The higher amount of synapsin I found in SC than in N and

T segments is in agreement with the suggestion that the role of synapsin I is more specific to the axon terminals than to the axon proper (De Camilli and Greengard, 1986). Furthermore, these findings agree with the immunochemical finding of a greater proportion of synapsin I in the terminal region than in the axon (De Camilli et al., 1983; Goldenring et al., 1986; Hirokawa et al., 1989). A longer period of residence time in the nerve terminals than in the axons has also been reported for synapsin I in rabbit retinal ganglion cells (Baitinger and Willard, 1987).

Posttranslational modification of synapsin I

The phosphorylation of synapsin I regulates its interaction with cytoskeletal elements and small synaptic vesicles *in vitro* (Schiebler et al., 1986; Bahler and Greengard, 1987; Petrucci and Morrow, 1987). Our results *in vivo* show that synapsin I transported with the SCb remains phosphorylated as it is transported along the axons (Fig. 2). We speculate that the phosphorylation of synapsin I could prevent actin filaments from forming a dense meshwork along the axon, which presumably could impair all axonal transport (McGuinness et al., 1989), and that it may facilitate the interaction of synapsin I with other cytomatrix components (Baines and Bennett, 1985, 1986; Petrucci and Morrow, 1987; Hirokawa et al., 1989). In fact, while phosphorylation inhibits the actin-bundling activity of synapsin I *in vitro,* it does not affect its ability to bind actin filaments and enhances the interaction with microtubules (Petrucci and Morrow, 1987).

It is relevant that a modification of phosphorylated synapsin I occurs at the nerve endings. In fact, a turnover of the initially incorporated radioactive phosphate groups after synapsin I has reached the nerve terminal compartment in the superior colliculus is suggested by the following evidence: (1) ^{32}P-labeled synapsin I was not detected 14 d after ^{32}P-orthophosphate injection, despite the fact that synapsin I accumulates at the terminals; (2) the disappearance in the SC segment of the more acidic α-forms detected in the axons; (3) the α-forms, but not the β-forms, were affected by alkaline phosphatase treatment; and (4) the portion of synapsin I dephosphorylated in the axon terminals is consistent with the fact that the purified synapsin I, that is, primarily dephosphorylated (Petrucci and Morrow, 1987), comprises only the β-forms. Dephosphorylation of transported synapsin I might be functional in determining the cytoarchitecture of the presynaptic terminals by clustering small synaptic vesicles to microfilaments. Although neuronal region–dependent change and time-dependent change in the electrophoretic resolution of synapsin I spots have previously been reported in the rabbit optic system (Baitinger and Willard, 1987), our data indicate that the change in spot morphology could be due to disappearance of the more phosphorylated forms of synapsin I.

In conclusion, the data presented here suggest that *in vivo* phosphorylation of axonally transported synapsin I may serve as a mechanism to regulate its interaction with cytomatrix components and synaptic vesicles. The bulk of synapsin I is axonally transported with the SCb of axonal transport, and it is phosphorylated at both the tail and head regions. Synapsin I phosphorylation at the tail region by CaM II may be active in preventing the formation of a dense F-actin meshwork, which would restrict organelle movement in the axoplasm. After synapsin I has entered the nerve endings, a change in its phosphorylation state occurs, which converts synapsin I axonal forms into nerve terminal forms. The overall decrease in the phosphorus content of synapsin I at specific sites in the terminals would allow synapsin I to cross-link small synaptic vesicles to actin filaments. Depolarization of the terminals promotes translocation of synapsin I from synaptic vesicles/cytoskeleton to cytosol (Sihra et al., 1989), thus modulating neurotransmitter release by controlling the availability of small synaptic vesicles. We do not yet know if, after synapsin I has reached the nerve endings, all sites are dephosphorylated. The role of the cAMP-dependent kinase phosphorylation of synapsin I is also unclear. The study of the phosphate turnover kinetics in the head and tail regions of the transported synapsin I after it has entered the nerve endings will possibly offer some insight into the mechanisms that cause synapsin I β-forms to predominate at the synaptic terminals.

References

Bahler M, Greengard P (1987) Synapsin I bundles F-actin in a phosphorylation-dependent manner. Nature 326:704–707.

Bahler M, Benfenati F, Valtorta F, Czernik AJ, Greengard P (1989) Characterization of synapsin I fragments produced by cystein-specific cleavage: a study of their interactions with F-actin. J Cell Biol 108: 1841–1849.

Baines AJ, Bennett V (1985) Synapsin I is a spectrin-binding protein immunologically related to erythrocyte protein 4.1. Nature 315:410–413.

Baines AJ, Bennett V (1986) Synapsin I is a microtubule-binding protein. Nature 319:145–147.

Baitinger C, Willard M (1987) Axonal transport of synapsin I–like proteins in rabbit retinal ganglion cells. J Neurosci 7:3723–3735.

Bonner WM, Laskey RJ (1974) A film detection method for tritium labelled proteins and nucleic acids in polyacrylamide gels. Eur J Biochem 46:83–88.

De Camilli P, Greengard P (1986) Synapsin I: a synaptic vesicle associated neuronal phosphoprotein. Biochem Pharmacol 35:4349–4357.

De Camilli P, Harris SM Jr, Huttern WB, Greengard P (1983) Synapsin I (protein I), a nerve terminal-specific phospho-protein. II. Its specific association with synaptic vesicles demonstrated by immunocytochemistry in agarose-embedded synaptosomes. J Cell Biol 96:1337–1354.

Fisher RA (1966) The design of experiments, 8th ed, pp 168–171, New York: Haffener.

Garner JA (1979) Cohesive movement of polypeptides characteristic of a distinct component of axonal transport. PhD thesis, Case Western Reserve University.

Garner JA, Lasek RJ (1982) Cohesive axonal transport of the slow component b complex of polypeptides. J Neurosci 2:1824–1835.

Goldenring JR, Lasher RS, Vollano DT, Ueda T, Stenberg NH, Stenberg LA, DeLorenzo RJ (1986) Association of synapsin I with the neuronal cytoskeleton. J Biol Chem 261:8495–8504.

Hirokawa N, Sobue K, Kanda K, Harada A, Yorifuji H (1989) The cytoskeletal architecture of the presynaptic terminal and molecular structure of synapsin I. J Cell Biol 108:111–126.

Huttner WB, DeGennaro LJ, Greengard P (1981) Differential phosphorylation of multiple sites in purified protein I by cyclic AMP–dependent and calcium-dependent protein kinases. J Biol Chem 256: 1482–1488.

Kennedy MB, Greengard P (1981) Two calcium/calmodulin-dependent protein kinases, which are highly concentrated in brain, phosphorylated protein I at distinct sites. Proc Natl Acad Sci USA 78: 1293–1297.

Laemmli UK (1970) Cleavage of structural proteins during the assembly of the head of bacteriophage T4. Nature 227:680–685.

Laskey RA, Mills AD (1975) Quantitative film detection of ^{3}H and ^{14}C in polyacrylamide gel fluorography. Eur J Biochem 57:335–341.

Llinas R, McGuinnes T, Leonard CS, Sugimori M, Greengard P (1985) Intraterminal injection of synapsin I or calcium/calmodulin dependent kinase II alters neurotransmitter release at the squid giant synapse. Proc Natl Acad Sci USA 82:3035–3039.

McGuinness TL, Brady ST, Gruner JA, Sugimori M, Llnas R, Greengard P (1989) Phosphorylation-dependent inhibition by synapsin I of organelle movement in squid axoplasm. J Neurosci 9:4138–4149.

O'Farrell PH (1975) High resolution two-dimensional electrophoresis of proteins. J Biol Chem 250:4004–4021.

Paggi P, Lasek RJ (1987) Axonal transport of cytoskeletal proteins in oculomotor axons and their residence times in the axon terminals. J Neurosci 7:2397–2411.

Paggi P, Lasek RJ, Katz MJ (1989) Slow component B protein kinetics in optic nerve and tract windows. Brain Res 504:223–230.

Paggi P, Lasek RJ, Katz MJ (1990) Cytomatrix protein residence times differ significantly between the tract and the terminal segments of optic axons. Brain Res 517:143–150.

Pearse BMF (1976) Clathrin: a unique protein associated with intracellular transfer of membrane by coated vesicles. Proc Natl Acad Sci USA 73:1255–1259.

Petrucci TC, Morrow JS (1987) Synapsin I: an actin-bundling protein under phosphorylation control. J Cell Biol 105:1355–1363.

Petrucci TC, Morrow JS (1991) The actin and tubulin binding domains of synapsin Ia and Ib. Biochemistry 30:413–422.

Petrucci TC, Mooseker MS, Morrow JS (1988) A domain of synapsin I involved with actin bundling shares immunologic cross-reactivity with villin. J Cell Biochem 36:25–35.

Schiebler W, Jahn R, Doucet JP, Rothlein J, Greengard P (1986) Characterization of synapsin I binding to small synaptic vesicles. J Biol Chem 261:8383–8390.

Sihra TS, Wang JKT, Gorelik FS, Greengard P (1989) Translocation of synapsin I in response to depolarization of isolated nerve terminals. Proc Natl Acad Sci USA 86:8108–8112.

Sudhof TC, Czernik AJ, Kao H-T, Takei K, Johnston PA, Horiuchi A, Kanazir SD, Wagner MA, Perin MS, De Camilli P, Greengard P (1989) Synapsin: mosaics of shared and individual domains in a family of synaptic vesicle phosphoproteins. Science 245:1474–1480.